

## Mechanism for zirconium oxide atomic layer deposition using bis(methylcyclopentadienyl)methoxymethyl zirconium

J. W. Elam<sup>a)</sup> and M. J. Pellin

Argonne National Laboratory, Argonne, Illinois 60439, USA

S. D. Elliott and A. Zydor

Tyndall National Institute, Lee Maltings, Cork, Ireland

M. C. Faia and J. T. Hupp

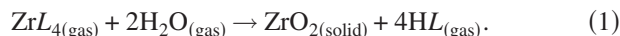
Department of Chemistry, Northwestern University, Evanston, Illinois 60208, USA

(Received 19 October 2007; accepted 22 November 2007; published online 20 December 2007)

The mechanism for zirconium oxide atomic layer deposition using bis(methylcyclopentadienyl)methoxymethyl zirconium and H<sub>2</sub>O was examined using *ab initio* calculations of hydrolysis energies to predict the order of ligand loss. These predictions were tested using *in situ* mass spectrometric measurements which revealed that the methyl ligand, and 65% of the methylcyclopentadienyl ligands are lost during the zirconium precursor adsorption. The remaining 35% of the methylcyclopentadienyl ligands and the methoxy ligand are lost during the subsequent H<sub>2</sub>O exposure. These measurements agree very well with the predictions, demonstrating that thermodynamic calculations are a simple and accurate predictor for the reactivities of these compounds. © 2007 American Institute of Physics. [DOI: 10.1063/1.2824814]

Atomic layer deposition (ALD) is a thin film growth method using alternating, self-limiting reactions between gaseous precursors and a solid surface to deposit materials in an atomic layer-by-layer fashion.<sup>1</sup> Zirconium oxide (ZrO<sub>2</sub>) is a promising high-dielectric constant replacement for SiO<sub>2</sub> in future microelectronic devices,<sup>2</sup> and also has applications in photovoltaics<sup>3</sup> and catalysis.<sup>4</sup> ALD is an attractive method for preparing ZrO<sub>2</sub> thin films because it affords precise thickness control and superb conformality.<sup>5</sup> Understanding the ALD mechanism is important because the mechanism affects the growth rate and purity of the films. Additionally, a mechanistic understanding can guide proper precursor selection. In this study, *ab initio* calculations are performed to predict the order in which the ligands are lost during ZrO<sub>2</sub> ALD. These predictions are tested using *in situ* quadrupole mass spectrometry (QMS).

We focus on the heteroleptic precursor, bis(methylcyclopentadienyl)methoxymethyl zirconium [Zr(MeCp)<sub>2</sub>(Me)(OMe)], abbreviated as ZrL<sub>4</sub>, with ligands L=MeCp, Me, and OMe. Heteroleptic precursors facilitate mechanistic studies and allow precursor fine tuning. The Zr and Hf versions of this precursor are thermally stable to 500 °C (Ref. 6) and produce high quality dielectric films.<sup>7</sup> Using H<sub>2</sub>O as oxygen source, the expected ALD reaction is



Equation (1) provides no information about the surface-mediated mechanism of growth or about the order of ligand release. This information is relevant because steric hindrance between the ligands remaining after the ZrL<sub>4</sub> pulse will dictate the ALD growth rate.<sup>8</sup>

At the start of the ZrL<sub>4</sub> pulse, the growing surface is covered with hydroxyls (surf-OH) that provide protons (H<sup>+</sup>). The adsorption of ZrL<sub>4</sub> produces ligands on the surface (L<sup>-</sup>=MeCp<sup>-</sup>, Me<sup>-</sup>, and OMe<sup>-</sup>), which can combine with pro-

tons and desorb as HL. The kinetics of this elimination reaction will be determined by the relative bond strengths<sup>9</sup> of Zr-L versus H-L at the surface, and by surface properties such as the O-H strength and H<sup>+</sup> diffusion rate. To compare different ligands, it is adequate to compute the different Zr-L versus H-L bond enthalpies and to ignore effects that are specific to surface geometry.<sup>10</sup>

We define the gas-phase Brønsted basicity (BB) of L<sup>-</sup> relative to OH<sup>-</sup> as

$$\Delta E_{\text{BB}} = \Delta E, \quad \text{for } L^- + \text{H}_2\text{O} \rightarrow \text{HL} + \text{OH}^-. \quad (2)$$

The more negative the ΔE<sub>BB</sub>, the stronger the BB of L<sup>-</sup> and the stronger the H-L bond. We compute the change in internal energy neglecting entropy/temperature effects. We likewise define the Lewis basicity (LB) of L<sup>-</sup> relative to OH<sup>-</sup> as

$$\Delta E_{\text{LB}} = \frac{1}{4}\Delta E, \quad \text{for } 4L^- + \text{Zr}(\text{OH})_4 \rightarrow \text{ZrL}_4 + 4\text{OH}^-. \quad (3)$$

Stronger Lewis bases with strong Zr-L bonding show more negative ΔE<sub>LB</sub>. Combining these equations, ΔE<sub>hyd</sub>=ΔE<sub>BB</sub>-ΔE<sub>LB</sub>, where

$$\Delta E_{\text{hyd}} = \frac{1}{4}\Delta E, \quad \text{for } \text{ZrL}_4 + 4\text{H}_2\text{O} \rightarrow \text{Zr}(\text{OH})_4 + 4\text{HL}. \quad (4)$$

Negative ΔE<sub>hyd</sub> corresponds to an exoergic hydrolysis reaction at T=0 K. ΔE<sub>hyd</sub> thus reflects the relative strengths of Zr<sup>4+</sup> and H<sup>+</sup> bonding to L<sup>-</sup>, using H<sub>2</sub>O and Zr(OH)<sub>4</sub> as common reference molecules. Equation (4) is thus a *model* reaction for HL elimination whenever surf-OH and surf-L are present. The resemblance of Eq. (4) to the overall growth reaction with H<sub>2</sub>O as precursor [Eq. (1)] is coincidental, since Eq. (1) contains no useful mechanistic information.

The species in Eq. (4) were modeled as isolated molecules in vacuum. The ground state electronic wavefunction of each molecule was calculated self-consistently within Kohn-Sham density functional theory (DFT) using TURBOMOLE (Ref. 11) with the B-P86 functional,<sup>12</sup> an atom-centered SV(P) basis set,<sup>18</sup> and a 28-electron effective core

<sup>a)</sup>Electronic mail: jelam@anl.gov.

TABLE I. Computed energies (kJ/mol) for ligands in model ALD reactions. The Brønsted basicity  $\Delta E_{\text{BB}}$  is from Eq. (2), the Lewis basicity  $\Delta E_{\text{LB}}$  from Eq. (3), and the hydrolysis energy  $\Delta E_{\text{hyd}} = \Delta E_{\text{BB}} - \Delta E_{\text{LB}}$  from Eq. (4). The ligand with the most negative  $\Delta E_{\text{hyd}}$  is predicted to be eliminated first.

| Ligand | Elimination product | $\Delta E_{\text{BB}}$ | $\Delta E_{\text{LB}}$ | $\Delta E_{\text{hyd}}$ |
|--------|---------------------|------------------------|------------------------|-------------------------|
| Me     | CH <sub>4</sub>     | -46.9                  | +176.6                 | -223.5                  |
| MeCp   | MeCpH               | +274.7                 | +375.1                 | -100.4                  |
| OMe    | MeOH                | +160.9                 | +152.5                 | +8.4                    |

potential on Zr.<sup>13</sup> All species were closed shell. Unconstrained optimization of the molecular geometry was carried out on the DFT potential energy hypersurface, but a vibrational analysis was not carried out. This method has been applied previously to heteroleptic Zr precursors.<sup>14</sup>

The calculated energetics are shown in Table I. The computed BB values decrease as MeCp > OMe > Me. The computed LB values are similar for Me and OMe but larger for MeCp. Applying Eq. (4),  $\Delta E_{\text{hyd}}$  increases as OMe > MeCp > Me. We therefore predict that Me ligands will be eliminated first during the ZrL<sub>4</sub> pulse, followed by MeCp ligands if there are sufficient surf-OH. The OMe ligands along with some MeCp should be eliminated during the H<sub>2</sub>O pulse.

To test these predictions, ZrO<sub>2</sub> ALD was monitored by QMS (Ref. 15) (Stanford Research Systems RGA300) in a viscous flow reactor<sup>16</sup> at 350 °C using alternating exposures to Zr(MeCp)<sub>2</sub>(Me)(OMe) (Epichem) for 3 s and de-ionized H<sub>2</sub>O for 1 s with 5 s purge periods between exposures. The Zr(MeCp)<sub>2</sub>(Me)(OMe) was vaporized at 95 °C. We verified that these conditions yield self-limiting ZrO<sub>2</sub> ALD using ellipsometric analysis of films deposited on silicon. The QMS signals arise from reactions occurring on the hot walls of the reactor, and no substrate is installed during these measurements.

The top three solid traces in Fig. 1 present the  $m/z=79$ ,  $m/z=16$ , and  $m/z=31$  QMS signals recorded during ZrO<sub>2</sub> ALD. The dotted lines at the bottom of the figure show the dosing times for the Zr(MeCp)<sub>2</sub>(Me)(OMe) and H<sub>2</sub>O precursors with a high value designating an exposure to the indicated precursor. The middle portion of the graph between 30 and 92 s shows 4½ ALD cycles in which the Zr(MeCp)<sub>2</sub>(Me)(OMe) and H<sub>2</sub>O precursors are pulsed sequentially. Between 0 and 30 s, only the Zr(MeCp)<sub>2</sub>(Me)(OMe) precursor is pulsed to measure the background for this compound. Similarly, only the H<sub>2</sub>O is pulsed between 92 and 120 s to evaluate the H<sub>2</sub>O background. Note that during the background measurements, both a 1 s exposure followed by a 5 s exposure are used to maintain the same timing sequence as in the ALD cycles.

During the ZrO<sub>2</sub> ALD cycles,  $m/z=31$  peaks are only observed during the H<sub>2</sub>O exposures and the corresponding background is small (~15%), indicating that the methoxy ligand (-OMe) is released exclusively during the H<sub>2</sub>O reaction. Similar results were obtained monitoring  $m/z=32$  in agreement with the cracking pattern for methanol<sup>17</sup> produced by the reaction of methoxy ligands with the hydroxylated surface.

The  $m/z=16$  trace in Fig. 1 shows the amount of CH<sub>4</sub> released during the ZrO<sub>2</sub> ALD along with the corresponding background measurements performed as described above. Peaks in the  $m/z=16$  signal are observed when dosing both the Zr(MeCp)<sub>2</sub>(Me)(OMe) and H<sub>2</sub>O precursors. However,

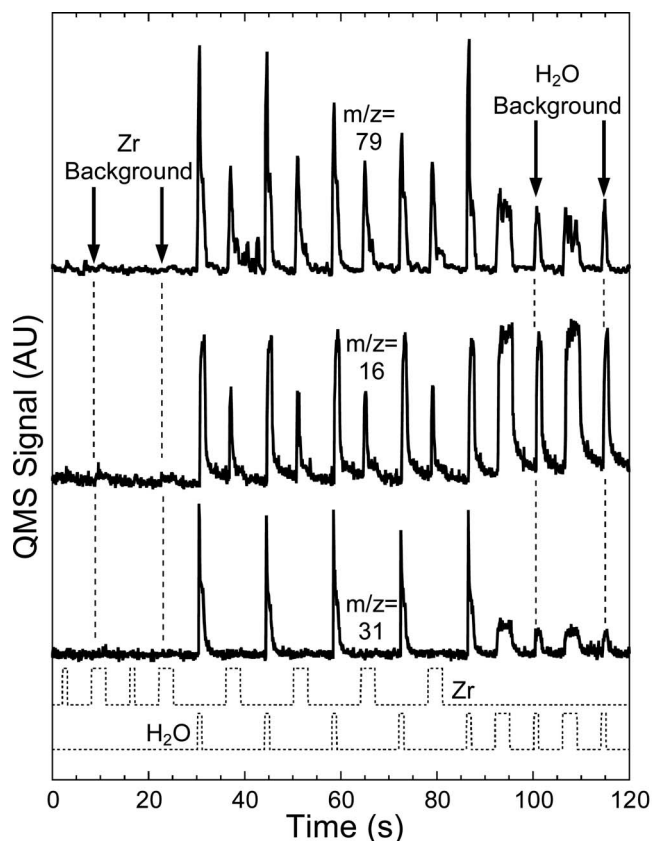


FIG. 1. QMS signals for  $m/z=31$  (MeOH),  $m/z=16$  (CH<sub>4</sub>), and  $m/z=79$  (MeCpH) measured during ZrO<sub>2</sub> ALD. The Zr(MeCp)<sub>2</sub>(Me)(OMe) and H<sub>2</sub>O doses are indicated by the dotted lines at the bottom. The Zr(MeCp)<sub>2</sub>(Me)(OMe) and H<sub>2</sub>O background signals are measured before and after the 4½, consecutive ZrO<sub>2</sub> ALD cycles as indicated.

while the Zr(MeCp)<sub>2</sub>(Me)(OMe) background is negligible at  $m/z=16$ , the H<sub>2</sub>O background and ALD signals are identical within the experimental error. Consequently, CH<sub>4</sub> is only released during the Zr(MeCp)<sub>2</sub>(Me)(OMe) exposures of the ZrO<sub>2</sub> ALD.

The  $m/z=79$  signals attributed to methylcyclopentadiene (MeCpH) formed during the ZrO<sub>2</sub> ALD in Fig. 1 reveal that MeCpH is released during both of the precursor exposures. Similar results were obtained using  $m/z=80$ , and 77 consistent with the cracking pattern for HCpMe.<sup>17</sup> Integration of the  $m/z=79$  peaks shows that, while the Zr(MeCp)<sub>2</sub>(Me)(OMe) background is negligible, 44% of the signal observed during the H<sub>2</sub>O exposures is background. After background correction, we conclude that 65(±10)% of the CpMe ligands are eliminated during the Zr(MeCp)<sub>2</sub>(Me)(OMe) exposures, and the remaining 35(±14)% are released during the subsequent H<sub>2</sub>O exposures.

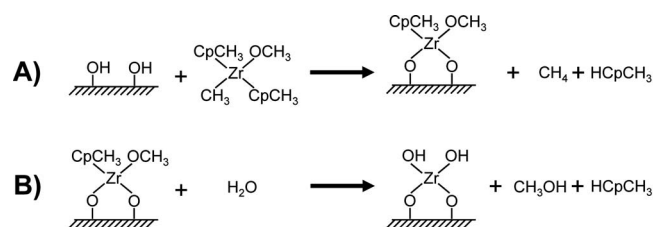


FIG. 2. Illustration of proposed ZrO<sub>2</sub> ALD mechanism.

The calculations and measurements suggest the mechanism for ZrO<sub>2</sub> ALD in Fig. 2. In step A, Zr(MeCp)<sub>2</sub>(Me)(OMe) reacts with the hydroxylated surface releasing the Me ligand as CH<sub>4</sub> and one or more of the MeCp ligands as MeCpH. This modified surface is exposed to H<sub>2</sub>O in step B, liberating any remaining MeCp ligands as MeCpH, and all of the OMe ligands as MeOH. The QMS measurements indicate that, on average, 1.3 MeCp ligands are removed in step A, so that 30% of the Zr(MeCp)<sub>2</sub>(Me)(OMe) molecules react with three hydroxyls and release both MeCp ligands in step A.

Following the Zr(MeCp)<sub>2</sub>(Me)(OMe) adsorption, the surface is covered with MeCp and OMe in the ratio ~2:3. Consequently, the steric bulk of these ligands will limit the ALD growth rate. However, because the Me ligand is eliminated before saturation, replacing the Me with a bulkier alkyl group should not affect the growth rate.

The QMS measurements follow the ligand release pattern suggested by the  $\Delta E_{\text{hyd}}$  calculations in Table I. This agreement supports our assertion that a simple comparison of bond strengths captures the essential information for predicting the ALD mechanism. Furthermore, we have identified the important precursor properties: strong affinity of Me for H<sup>+</sup> of surf-OH, weak bonding of MeCp to Zr, and similar bonding of OMe to Zr and H.

The submitted manuscript has been created by the University of Chicago—Argonne, LLC as Operator of Argonne National Laboratory (“Argonne”) under Contract No. DE-AC02-06CH11357 with the U.S. Department of Energy. The work at Northwestern is supported by the U.S. Department of Energy, Basic Energy Sciences Program under Grant No. DE-FG02-87ER13808. The work at Tyndall was supported by the European Commission under the sixth Framework project REALISE (NMP4-CT-2006-016172, <http://www.tyndall.ie/realise>).

- <sup>1</sup>M. Ritala and M. Leskelä, in *Handbook of Thin Film Materials*, edited by H. S. Nalwa (Academic, San Diego, 2001), Vol. 1, p. 103.
- <sup>2</sup>G. D. Wilk, R. M. Wallace, and J. M. Anthony, *J. Appl. Phys.* **89**, 5243 (2001).
- <sup>3</sup>D. B. Menzies, Q. Dai, L. Bourgeois, R. A. Caruso, Y. B. Cheng, G. P. Simon, and L. Spiccia, *Nanotechnology* **18**, 125608 (2007).
- <sup>4</sup>A. Woosch, C. Descorme, S. Rousselet, D. Duprez, and C. Ternplier, *Appl. Surf. Sci.* **253**, 1310 (2006); C. P. Nicholas and T. J. Marks, *Langmuir* **20**, 9456 (2004).
- <sup>5</sup>K. Kukli, M. Ritala, J. Aarik, T. Uustare, and M. Leskelä, *J. Appl. Phys.* **92**, 1833 (2002); M. Putkonen, J. Niinistö, K. Kukli, T. Sajavaara, M. Karppinen, H. Yamauchi, and L. Niinistö, *Chem. Vap. Deposition* **9**, 207 (2003); K. Kukli, J. Niinistö, A. Tamm, J. Lu, M. Ritala, M. Leskelä, M. Putkonen, L. Niinistö, F. Song, P. Williams, and P. N. Heys, *Microelectron. Eng.* **84**, 2010 (2007).
- <sup>6</sup>S. Rushworth, K. Coward, H. Davies, P. Heys, T. Leese, L. Kempster, R. Oedra, and P. Williams, *Surf. Coat. Technol.* **201**, 9060 (2007).
- <sup>7</sup>J. Niinistö, M. Putkonen, L. Niinistö, F. Q. Song, P. Williams, P. N. Heys, and R. Oedra, *Chem. Mater.* **19**, 3319 (2007).
- <sup>8</sup>R. L. Puurunen, *Chem. Vap. Deposition* **9**, 249 (2003).
- <sup>9</sup>Although reaction rates are governed by activation energies rather than bond enthalpies, the relative activation energies are likely to follow the same trends as bond enthalpies in this set of similar reactions.
- <sup>10</sup>S. D. Elliott, *Surf. Coat. Technol.* **201**, 9076 (2007).
- <sup>11</sup>R. Ahlrichs, M. Bär, M. Häser, H. Horn, and C. Kölmel, *Chem. Phys. Lett.* **162**, 165 (1989).
- <sup>12</sup>A. D. Becke, *Phys. Rev. A* **38**, 3098 (1988); J. P. Perdew, *Phys. Rev. B* **33**, 8822 (1986).
- <sup>13</sup>D. Andrae, U. Haussermann, M. Dolg, H. Stoll, and H. Preuss, *Theor. Chim. Acta* **77**, 123 (1990).
- <sup>14</sup>A. Zydor, S. D. Elliott, T. Leese, F. Song, and S. Rushworth, *ECS Trans.* **11**, 113 (2007).
- <sup>15</sup>J. Niinistö, A. Rahtu, M. Putkonen, M. Ritala, M. Leskelä, and L. Niinistö, *Langmuir* **21**, 7321 (2005); A. Rahtu and M. Ritala, *J. Mater. Chem.* **12**, 1484 (2002).
- <sup>16</sup>J. W. Elam, M. D. Groner, and S. M. George, *Rev. Sci. Instrum.* **73**, 2981 (2002).
- <sup>17</sup>*Eight Peak Index of Mass Spectra* (Mass Spectrometry Data Centre, The Royal Society of Chemistry, Cambridge, UK, 1991), Vol. 1, p. 1.
- <sup>18</sup>A. Schäfer, H. Horn, and R. Ahlrichs, *J. Chem. Phys.* **97**, 2571 (1992); K. Eichkorn, F. Weigend, O. Treutler, and R. Ahlrichs, *Theor. Chem. Acc.* **97**, 119 (1997).